

A Second Look at the Second Beta Test	579
Diophantine Equations and the Parking Problem	596
What Type of Apollonian Circle Packing Will Appear?	611
Quadrilateral Centers and the Pappus Equation	630
Discrepancy of Quaternions Generalized	640
NOTES	
Centroid of Three Area-Bisecting Centers of a Triangle	648
An Algebraic Proof of Fermat's Last Theorem	652
The Power of the Half Power	655
PROBLEMS AND SOLUTIONS	
REVIEWS	
The Logic of Combinatorics by Eric Brown and Richard Coe	667
MAFIBITE	
1921 The Digital Analysis of the Proof of Fermat's Last Theorem by Andrew Wiles	

ISSN: (Print) (Online) Journal homepage: <https://maa.tandfonline.com/loi/uamm20>

What Type of Apollonian Circle Packing Will Appear?

Jan E. Holly

To cite this article: Jan E. Holly (2021) What Type of Apollonian Circle Packing Will Appear?, The American Mathematical Monthly, 128:7, 611-629, DOI: [10.1080/00029890.2021.1933834](https://doi.org/10.1080/00029890.2021.1933834)

To link to this article: <https://doi.org/10.1080/00029890.2021.1933834>



Published online: 06 Aug 2021.



Submit your article to this journal [↗](#)



Article views: 461



View related articles [↗](#)



View Crossmark data [↗](#)

What Type of Apollonian Circle Packing Will Appear?

Jan E. Holly 

Abstract. An Apollonian circle packing is created by starting with three pairwise tangent circles, adding the two circles—or circle and line—tangent to the first three, then repeating the process forever by successively adding new circles and lines tangent to every new tangent threesome of circles and/or lines. The resulting packing is one of four types: bounded (enclosed by one of the circles), half-plane (with one line), strip (with two lines), or full-plane. Given three starting circles, what type of Apollonian circle packing will appear? This article gives an answer in the form of a picture, i.e., a plot in the parameter space of relative sizes of the starting circles, indicating the types of packings. The result is a fractal, which is then further explored.

1. THE PROBLEM. Draw three circles that are pairwise externally tangent. Then draw the two circles, or circle and line, that are tangent to all of the first three. Notice that the “outside circle” either surrounds the first three, is a line instead of a circle, or is externally tangent to the first three, as in [Figure 1](#).

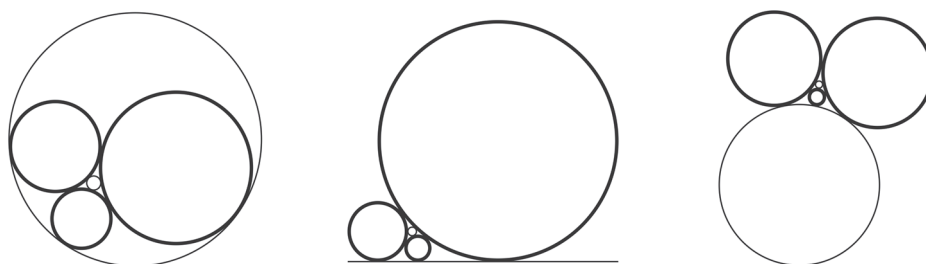


Figure 1. Possible arrangements of the next two tangent circles (thin), or circle and line, given three tangent circles (thick).

Now, for each newly existing threesome of pairwise tangent circles and/or lines, draw the missing circle or line that is tangent to all three. Repeating this process forever makes an *Apollonian circle packing* that is either *bounded*, *half-plane*, *strip*, or *full-plane*, as shown in [Figure 2](#). Note that parallel lines are considered tangent at infinity.

What type of packing will appear when starting with a given three circles? Surely, “most” of the time, a bounded packing will appear. Particularly intriguing is a full-plane packing, whose existence is not immediately obvious in the first place. Nevertheless, as explained in [Section 2](#), all four types of packing are known to be possible, but a definitive test for determining the resulting type is surprisingly elusive.

The goal of this article is to produce an answer in the form of a picture. The development of a picture leads to new results and a way to visualize the answer, even though infinite precision would be required in order for the picture to be a definitive test.

doi.org/10.1080/00029890.2021.1933834

MSC: Primary 52C26, Secondary 14H50; 28A80

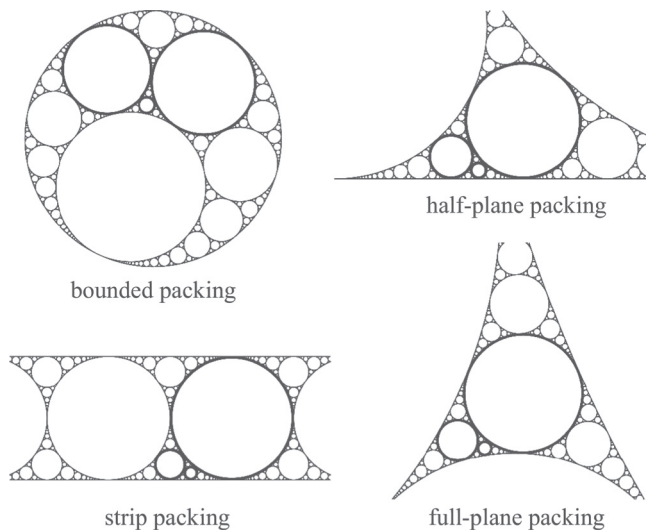


Figure 2. The four types of Apollonian circle packings. For all except the bounded packing, only a small piece is shown; circles are chopped off at the edges of the images, and infinitely many more circles exist in the directions indicated by the name of the type of packing. The bounded packing illustrated here arises from the rightmost example of Figure 1, and the strip packing arises from the middle example of Figure 1.

Above all, the goal is to have some fun, and create a playground for additional inquiry and exploration.

Because the type of packing depends solely on the relative sizes of the starting circles, some terminology is helpful. To facilitate phrasing of the new results, *circle* will mean an actual circle, not a line, although some results will apply equally to lines or can be extended to include lines.

Definitions. For purposes of this article, a *trio* is a set of three pairwise externally tangent circles. If $r_1 \geq r_2 \geq r_3$ are the radii of the circles, then the *ratio pair* of the trio is $(r_2/r_1, r_3/r_2) \in (0, 1] \times (0, 1]$. A *triple* is the same as a trio but allows one of the circles to instead be a line, in which case the *ratio pair* is $(0, r_3/r_2)$ where $r_2 \geq r_3$ are the radii of the circles.

Triples with the same ratio pair obviously generate packings that are equivalent under similarity, i.e., under compositions of translations, reflections, rotations, and/or scalings. Therefore, a ratio pair is said to generate a bounded, strip, half-plane, or full-plane packing if a triple with that ratio pair does.

Because a triple's ratio pair determines the type of packing, the picture answer developed in this article will be a plot of the unit square of ratio pairs, indicating which ratio pairs correspond to which of the four types of packings in Figure 2. Presented here are two complementary approaches to the development of the plot, which is displayed in Figure 6. The first approach—presented in Sections 3 and 4—is the more constructive one, requires no previous background, and suggests new avenues for exploration. The second approach—outlined in Section 5—comes from the viewpoint of projective geometry, and provides an understanding of the general structure of the picture answer. It is possible to skip Section 5, jumping straight into the exploration in Section 6, which takes a closer look at the result, and gives ideas for further exploration. Prior to both approaches, Section 2 provides relevant background.

2. KNOWN FACTS. An important ingredient in the study of Apollonian packings is the relationship between the radii of the tangent circles. A nice formula exists using curvature ($= 1/\text{radius}$). For a triple with curvatures a , b , and c , the curvatures of the two circles—or circle and line—tangent to the triple are given by

$$d = a + b + c \pm 2\sqrt{ab + ac + bc}, \quad (1)$$

where negative curvature means that the circle surrounds the triple. Proving this formula is not as easy as it looks. The reader is welcome to try, or to look at various proofs such as those in [17, 23, 24] and [7, pp. 14–15], which use a symmetric version that can be stated as follows.

Descartes Circle Theorem. *For a triple with curvatures a , b , and c , the curvatures of the two circles—or circle and line—tangent to the triple are the values of d that satisfy*

$$2(a^2 + b^2 + c^2 + d^2) = (a + b + c + d)^2. \quad (2)$$

By symmetry in this equation and by allowing negative curvature, (1) and (2) can be used for all arrangements of tangent circles and lines that appear in an Apollonian packing. For delightful expositions of the history, see [6, 18, 25]; for the Descartes portion of the history, see also [2] for a discussion of the role that the work of Princess Elisabeth Simmern van Pallandt of Bohemia played in Descartes's proof.

Bounded packings are the most studied type. This is partly because they are fun to draw, but also due to the fascinating fact that infinitely many different bounded packings can be created using only integer curvatures. Integral Apollonian packings whose circles' curvatures have greatest common divisor 1 are called *primitive integral Apollonian packings* by the authors of [11], who classified them and pointed out that the only unbounded primitive integral Apollonian packing is the strip packing with largest circles having radius 1. (This fact can be seen geometrically, as explained in the discussion about properties after Proposition 2.1, considering that every integral packing is equivalent by scaling to a primitive integral packing.) Underlying the work on integral packings is the observation that for the two solutions, d_1 and d_2 , to (1),

$$d_1 + d_2 = 2a + 2b + 2c. \quad (3)$$

Therefore, by starting with *four* pairwise tangent circles and/or lines, all curvatures in the packing can be calculated by systematic application of (3), which implies that integer curvatures lead to integer curvatures. Mathematicians have pounced upon this enticing fact, producing questions and results too numerous to discuss here. A nice introduction is given in [25], and more extensive surveys can be found in [3, 10, 15, 22].

The fact that an integral Apollonian packing must be either bounded or a strip packing implies the following, stated in the terminology of the present article.

Proposition 2.1. *If triple T has ratio pair (x, y) with $x, y, \sqrt{xy^2 + xy + y} \in \mathbb{Q}$, then the Apollonian packing generated by T is either a bounded packing or a strip packing.*

Proof. Given such a triple T , let $a \leq b \leq c$ be the curvatures of the members of T , so $(x, y) = (a/b, b/c)$. Scaling by $1/c$ gives a triple with curvatures $a/c = xy$, $b/c = y$, and 1. From this triple, equation (1) and the hypothesis of the proposition show that the set consisting of T and a fourth tangent circle or line is equivalent by scaling to a set of four with rational curvatures. Equation (2) implies that scaling again can give a set of four with integer curvatures, which therefore generates either a bounded packing or a strip packing. ■

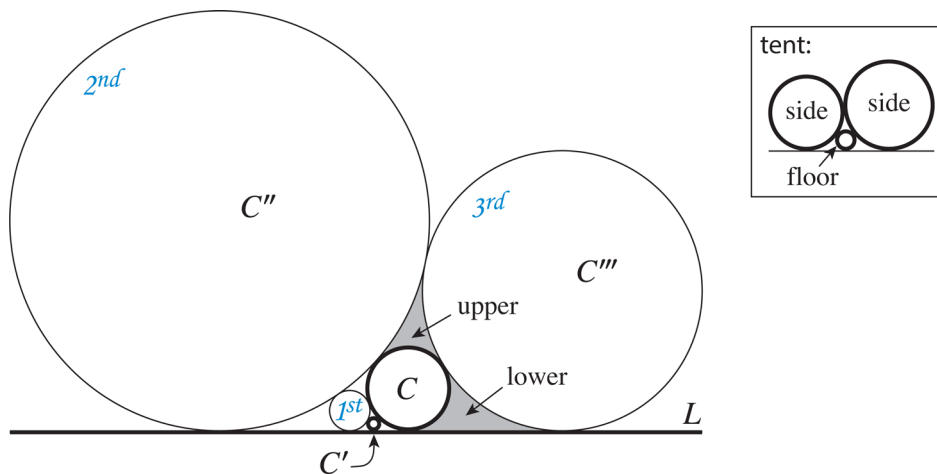


Figure 3. Starting with $\{C, C', L\}$, example of successive circles — 1st, 2nd, 3rd — that are tangent to L to the left or right of the circles so far. Such a process continues forever unless a second line appears due to the two largest circles having the same radius. Circles labeled C'' and C''' are used in the proof of Lemma 3.2 to illustrate the creation of a tent with floor C . (Tents are discussed in Section 3.) The curvilinear triangles labeled “upper” and “lower” are used in the proof of Lemma 3.3 to show possible locations of a circle D .

It turns out that there is only one strip packing up to similarity. This can be deduced from properties of the constructions of packings, explained here using additional terminology.

Definitions. The circles in the initial trio comprise the 0th generation. For each $n > 0$, the n th generation is composed of all new circles and/or lines tangent to the triples so far, i.e., up through the $(n - 1)$ st generation.

Surrounded by a triple means “contained in the solid, closed triangle whose vertices are the points of intersection of the members of the triple.”

The *outside circle* for a triple is the circle tangent to the members of the triple but not surrounded by the triple. Some triples do not have an outside “circle” because they have a line that is tangent instead.

A property that holds through certain generations of a construction of a packing is the existence of a surrounding triple after each generation. For example, in the 1st generation, if the outside circle for the initial trio is externally tangent as in the right-most example of Figure 1, then there is a trio that surrounds all of the other circles up through the 1st generation. This property clearly perpetuates itself: For each successive generation in which the outside circle for the previous generation’s surrounding triple is externally tangent to that trio, there is a new trio that surrounds all of the other circles up through the current generation. This behavior can be seen, for example, by starting with any trio in the full-plane packing of Figure 2.

Next, if a (first) line appears, then that line becomes part of a surrounding triple for the packing through the current generation. This property of having a surrounding triple perpetuates itself through subsequent generations that do not produce a second line. Figure 3 illustrates the addition of new outside circles.

As a side effect, these sequences of surrounding trios and triples cause full-plane and half-plane packings to have increasingly larger circles and therefore nonintegral curvatures, proving that only bounded and strip packings can be integral as mentioned above in the discussion about bounded packings.

To obtain a strip packing, the second line can appear only by being tangent to the surrounding triple of the previous generation, which means that the triple’s two circles

must be the same size. Such a packing can also be generated by starting with those two circles and a line, a fact mentioned later (Fact 3.1), so all strip packings are equivalent. Thus, Proposition 2.1 has a converse for strip packings.

Proposition 2.2. *If triple T with ratio pair (x, y) generates a strip packing, then $x, y, \sqrt{xy^2 + xy + y} \in \mathbb{Q}$.*

Proof. Given such a triple T , let $a \leq b \leq c$ be the curvatures of the circles and/or line. Because this triple's packing is equivalent to the primitive integral strip packing, the integral strip packing can be generated by a triple whose members have curvatures $sa, sb, sc \in \mathbb{Z}$ for some $s \in \mathbb{R}$. Clearly, $x, y \in \mathbb{Q}$. Next, equation (1) with sa, sb , and sc in place of a, b , and c , respectively, must give integer values for d because all circles in the integral packing have integer curvatures. Dividing by sc leads to $\sqrt{xy^2 + xy + y} \in \mathbb{Q}$. ■

A related result was provided by Ching and Doyle [4] who considered pairs of tangent circles tangent to a line. In that context, the main result was a complete classification of half-plane packings up to equivalence, and one corollary was the following distinction between strip and half-plane packings.

Proposition 2.3. *Let T be a triple with ratio pair $(0, y)$. Then T generates a strip packing if and only if $\sqrt{y} \in \mathbb{Q}$.*

Proof. For a triple T with ratio pair $(0, y)$, if $\sqrt{y} \in \mathbb{Q}$ then Proposition 2.1 implies that the packing generated by T must be a strip packing because a bounded packing has no line and thus no triple with ratio pair $(0, y)$.

The converse follows from Proposition 2.2. ■

Half-plane and full-plane packings require irrational curvatures. This is because any subset of four pairwise tangent circles with rational curvatures is equivalent by scaling to a set with integer curvatures, which leads to an integral packing. Do half-plane and full-plane packings even exist? The answer is “yes,” most immediately because self-similar packings can be generated by starting with carefully chosen curvatures. For example, one self-similar half-plane packing stems from curvatures $a = 0, b = \phi + 1$, and $c = 1$, where $\phi = \frac{1+\sqrt{5}}{2}$ is the golden ratio. Self-similarity is quickly apparent by looking at the successively larger circles that appear on alternating sides of the circles with curvatures b and c . The next circle has curvature $d = \frac{1}{\phi+1}$ as confirmed by (2), so $d/c = c/b$ which gives a scaled symmetry that repeats forever as larger circles are added on alternating sides. This half-plane packing is shown in Figure 2.

A self-similar full-plane packing can be generated by letting $a = 1$ and solving (2) for b and c with conditions $b = c/b = d/c$. This equation can be solved by writing c and d in terms of b , and then rearranging and factoring:

$$(b^2 - (1 + \sqrt{5})b + 1)(b^2 - (1 - \sqrt{5})b + 1)(b^2 + 1) = 0.$$

Only the first factor has real roots. Choosing the solution $b = \phi - \sqrt{\phi} < a = 1$ gives $a > b > c > d$ and successively larger circles spiraling outward. This full-plane packing is shown in Figure 2. Other self-similar half-plane and full-plane packings can also be created.

3. TENTS. The pursuit of a picture begins with new definitions that lead to uniqueness results. This section focuses primarily on situations in which a line exists, because half-plane and strip packings provide the framework in Section 4 for the development of a picture.

Definitions. A *tent* is a trio for which there exists a line tangent to all three circles. The smallest circle is the *floor* of the tent, and the other two circles are the *sides* of the tent, as illustrated in Figure 3. In an Apollonian packing generated by a tent, a circle or set of circles is *inside* the tent if it is in the interior of the triangle whose vertices are the points of tangency of the members of the tent, and a *tent collection* is the set of circles consisting of a tent and the circles inside the tent.

The proofs assume the ability to visualize the geometry of tents, as well as the manner in which circles become arranged when generating an Apollonian packing. Also used implicitly is the following fact:

Fact 3.1. *In an Apollonian packing, any set of three pairwise tangent circles and/or lines would produce that same packing.*

A direct way to prove this is by finite induction on the generations during construction of a packing, using the symmetry of (2) to show that any set of three tangent circles and/or lines in the packing will eventually produce the three from which the packing was originally generated. Another proof is given in [4], making use of the fact that the complement of the union of open disks associated with the circles in an Apollonian packing has Lebesgue measure zero [12, 14]. Alternatively, a proof could appeal to the *Apollonian group* generated by 4×4 matrices stemming from (2) and acting on quadruples of curvatures, introduced by Hirst [13] with subsequent elaboration and results in [1, 11]. The Apollonian group involves only curvatures, but positions can be addressed by using results in [16] about the circles' centers.

Lemma 3.2. *In a half-plane or strip packing, each circle C tangent to exactly one line is the floor of a unique tent, and the sides of the tent are the two largest circles tangent to C .*

Proof. Fix a half-plane or strip packing, and let C be a circle tangent to exactly one line, L . By choosing a circle C' in the packing tangent to both L and C , construction of the Apollonian packing from $\{L, C, C'\}$ will lead as in Figure 3 to a circle C'' (which may be C') that is on the same side of C as C' , is tangent to both C and L , and is larger than C ; the existence of such a C'' is perhaps geometrically intuitive, but also can be deduced from equation (1). The construction then leads to a circle C''' on the other side of C that is larger than C and tangent to all of C'', C , and L . Therefore, $\{C, C'', C'''\}$ is a tent with floor C . It is clear from the construction and nature of an Apollonian packing that C'' and C''' are the only two circles tangent to and larger than C , so C cannot be the floor of another tent. ■

Lemma 3.3. *In a half-plane or strip packing:*

- (a) *Each circle not tangent to a line is inside exactly one tent (and therefore is a member of exactly one tent collection).*
- (b) *Each trio is contained in exactly one tent collection.*

Proof. Fix a half-plane or strip packing.

(a) Let D be a circle that is not tangent to a line. Let L be the line, or the closest line in the case of a strip packing, since D clearly cannot be inside a tent tangent to the other line due to the arrangement of circles and lines (as in Figure 2). Consider L to be across the bottom of the packing.

Choose a triple $\{C, C', L\}$ from which to construct the packing again; Figure 3 serves as an example. If $\{C, C', L\}$ does not surround D (imagining D in its place in

the completed packing), then successively add circles to the left and/or right of the circles so far, in a similar procedure to that in Figure 3, until D is surrounded by a triple. The circle that causes D to finally be surrounded, say C''' in Figure 3 for illustrative purposes, places D in either an upper or a lower curvilinear triangle. In the former case, D is inside a tent such as $\{C, C'', C'''\}$ in Figure 3. In the latter case, or in the case that D is surrounded by the original triple $\{C, C', L\}$, successively add smaller circles tangent to L in the latest curvilinear triangle containing D until one of those circles is the floor of a tent with D inside.

Call the tent T and the floor F . To prove uniqueness of this tent, suppose for contradiction that D is inside another tent T' with floor F' . By Lemma 3.2, $F' \neq F$. By the geometry of tents, every vertical line segment between D and L must intersect the floor F' . Therefore, F' is tangent to L between F and a side of T ; for example, if $T = \{C, C'', C'''\}$ in Figure 3, then F' is in either the “lower” curvilinear triangle or that between C'', C , and L . However, this means that T' cannot extend past F and that side of T , so D cannot be inside T' .

(b) Given a trio U , if U is a tent, then it is clearly contained in only its own tent collection. Otherwise, let $S \neq \emptyset$ consist of the members of U not tangent to a line. By (a), each member of S is inside exactly one tent. The tangency of members of S implies that they are all inside the same tent, say T with associated line L . It follows that U is contained in the tent collection of T because each member of $U \setminus S$ is tangent to each member of S , and the only circles tangent to both L and circles inside T are the members of T . Uniqueness follows from (a). ■

Lemma 3.4. *Within a given tent collection, for each trio T there is at most one other trio with the same ratio pair as T . If the tent is asymmetric, i.e., the sides’ radii are not equal, then no two trios contained in the tent collection have the same ratio pair.*

Proof. Suppose that trios T_1, T_2 , and T_3 have the same ratio pair and are contained in the tent collection of tent $\{A, B, C\}$. Because T_1 and T_2 have the same ratio pair, there is a similarity transformation taking T_1 to T_2 and the packing bijectively to itself. Similarity transformations map tent collections to tent collections, so Lemma 3.3(b) implies that T_1 ’s tent collection maps to T_2 ’s tent collection; thus $\{A, B, C\}$ maps to itself. If the tent is asymmetric, then the transformation must be the identity, so $T_1 = T_2$, and by a similar argument, $T_1 = T_3$. If the tent is symmetric, then the only other possible transformation is the reflection that swaps the sides of the tent. Therefore, considering both transformations from T_1 to T_2 and from T_1 to T_3 , at least two of T_1, T_2 , and T_3 must be equal. ■

Definition. The *tent ratio pair* of a trio T is the ratio pair of the tent whose tent collection contains T . The *tent ratio pair* of a ratio pair P is the same as that of a trio with ratio pair P .

Theorem 3.5. *There is a one-to-one correspondence between the following two sets.*

- I: The set of ratio pairs of trios that generate a half-plane or strip packing, excluding those with tent ratio pair $(1, 1/4)$.*
- J: The set of trios of circles that are in a tent collection of a tent $\{A(t), B, C(t)\}$ with floor $C(t)$ as shown in Figure 4, where the sides $A(t)$ and B have curvatures $t \in (0, 1)$ and 1, respectively.*

Proof. It suffices to show that the map from J to I taking each trio to its ratio pair is one-to-one and onto.

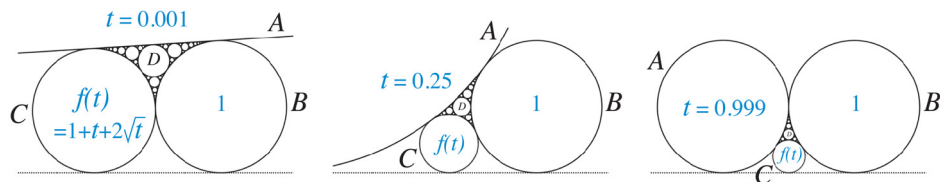


Figure 4. The parametrized set of tent collections for [Theorem 3.5](#). Circles $A(t)$, B , and $C(t)$ are tangent to the horizontal line, and all circles except B are parametrized by the curvature t of $A(t)$. The curvature $f(t)$ of the tent's floor $C(t)$ is determined by equation (1).

First, notice that every possible ratio pair of a tent, with the exception of $(1, 1/4)$, is realized by $\{A(t), B, C(t)\}$ for exactly one value of $t \in (0, 1)$ because a tent's ratio pair (x, y) is determined by its sides, and every value $x \in (0, 1]$ appears here except $x = 1$ which corresponds to $(x, y) = (1, 1/4)$.

To show that the map is one-to-one, suppose for contradiction that distinct trios T_1 and T_2 in J have the same ratio pair. Then T_1 and T_2 have the same tent ratio pair, and therefore the same tent, $\{A(t), B, C(t)\}$ for some t . This contradicts [Lemma 3.4](#).

To show that the map is onto, consider a ratio pair P in I . Let T be a trio with ratio pair P , and in the packing generated by T let T' be the tent whose tent collection contains T . Let P' be the ratio pair of T' . By definition of I , $P' \neq (1, 1/4)$, so let t be such that $\{A(t), B, C(t)\}$ has ratio pair P' . The packings generated by T' and by $\{A(t), B, C(t)\}$ are then equivalent by a similarity transformation, and because T is contained in the tent collection of T' , its image, T'' , is contained in the tent collection of $\{A(t), B, C(t)\}$. Therefore T'' , which has the same ratio pair as T , is a member of J and has ratio pair P . ■

4. THE PICTURE. The key to developing a picture is to recognize that half-plane and strip packings constitute borderline cases: Any triple in these packings is on the brink of producing a bounded packing instead. A slight nudge of the circle sizes may cause a line to curve inward and become a circle enclosing the packing. Triples in strip packings, especially, teeter on a knife's edge, with almost any nudge causing one of the lines to enclose the packing.

More formally, ratio pairs that generate bounded packings form an open set in $[0, 1] \times (0, 1]$, and the boundary of the open set consists of the ratio pairs that generate half-plane and strip packings. If a plot displays that boundary, and if the open set for bounded packings is thereby indicated, then all remaining ratio pairs in $[0, 1] \times (0, 1]$ generate full-plane packings. If the strip-packing ratio pairs can somehow be distinguished from the half-plane packing ratio pairs on the bounded-packing boundary, then the plot is a picture answer to the question of which type of packing will appear from which starting triples.

The initial development of the plot is shown in [Figure 5](#). Each curve is the parametric curve of the ratio pair as a function of t for a parametric trio in [Figure 4](#). For example, the curve for parametric trio $\{A(t), B, C(t)\}$ is given by

$$x(t) = t$$

$$y(t) = 1/(1 + t + 2\sqrt{t}).$$

Each additional curve uses the relevant circles' curvatures as determined by equation (1) when generating the tent collection starting with $\{A(t), B, C(t)\}$. Because each trio in [Figure 4](#) leads to one new tangent circle and thus three new trios, there is, in effect, a ternary tree of trios and therefore of parametric curves. The plots in [Fig-](#)

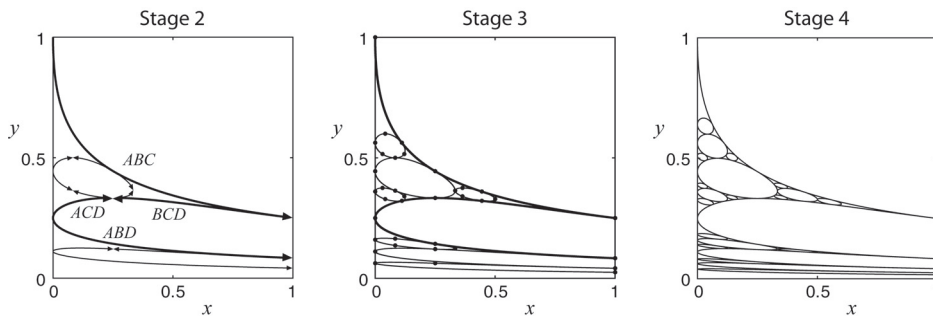


Figure 5. Ratio pairs that generate half-plane and strip packings. The Stage 2 graph shows the parametric curves of ratio pairs of triples in Figure 4 up through the 2nd generation of circles, considering the 0th generation to be $\{A(t), B, C(t)\}$. Arrowheads are at $t = 1$ on each curve. Parametric curves for the four triples up through the 1st generation of circles are labeled by the triples, omitting “(t)” for ease of display. (The curve BCD begins at $x = 1$; the other three begin at $x = 0$.) The Stages 3 and 4 graphs show the parametric curves of the ratio pairs of triples involving circles up through the 3rd and 4th generation, respectively. Dots in the Stage 3 graph indicate the intersections of curves, thereby identifying some ratio pairs that generate strip packings.

ure 5 were developed in MATLAB [19] by coding this ternary tree. Upon seeing the plots, deciphering the relationship between positions of trios in Figure 4 and locations of curves in Figure 5 turns out to be quite a puzzle, and a thorough labeling is not attempted here. Instead, an investigation into the pattern of placements of curves provides an intriguing topic for further exploration, as discussed in Section 6.

Technically, Figure 4 uses only t such that $0 < t < 1$, but the curves’ endpoints provide additional information, so consider also $t \in \{0, 1\}$. First, triples with $t = 0$ or $t = 1$ clearly generate strip packings. Also quite relevant is the *nonuniqueness* of these triples in correspondence to ratio pairs, unlike those in Theorem 3.5 which has $0 < t < 1$. For triples with $t = 0$ or $t = 1$, every triple except $\{A(0), B, C(0)\}$ has at least one other triple with the same ratio pair among the triples with $t = 0$ or $t = 1$, possibly both. These matchings are discussed further in Section 6. In addition, many such triples share a ratio pair with a triple among those with $0 < t < 1$. For example, the $t = 0$ triple of B, D , and the next circle between A, B , and D has the same ratio pair as the $t = 0.25$ triple of A, B , and C . An important consequence of the nonuniqueness of these triples is that intersections of curves in the plot indicate ratio pairs that generate strip packings (which are all equivalent).

Note that these curves are pieces of algebraic curves. This follows from the fact that the parametric equations are obtained by successively applying equation (1) to curvatures as functions of t , and taking ratios. Therefore, equations for algebraic curves can be obtained by creating pairs of polynomial equations (e.g., $x - t = 0$ and $4y^2t - (1 - y - yt)^2 = 0$ for the equations above for $\{A(t), B, C(t)\}$) and then finding resultants [5] of the pairs of polynomials considered as polynomials in t in order to eliminate t .

Figure 6 shows the final picture answer, created by continuing the process described for Figure 5. Strip packings are given by the points—i.e., ratio pairs—at the countably infinite number of intersections of curves, and at $(0, 1)$. Half-plane packings are given by the other points on the curves and y -axis. Bounded and full-plane packings are given by the remaining points, as discussed next.

Ratio pairs in the oval-shaped regions delineated by the curves give bounded packings, as do those in the partial-oval regions that stretch to $x = 1$. These facts can be deduced to a certain extent by looking at various curves and their associated triples in

Type of Apollonian Circle Packing as a Function of Ratio Pair (x, y)

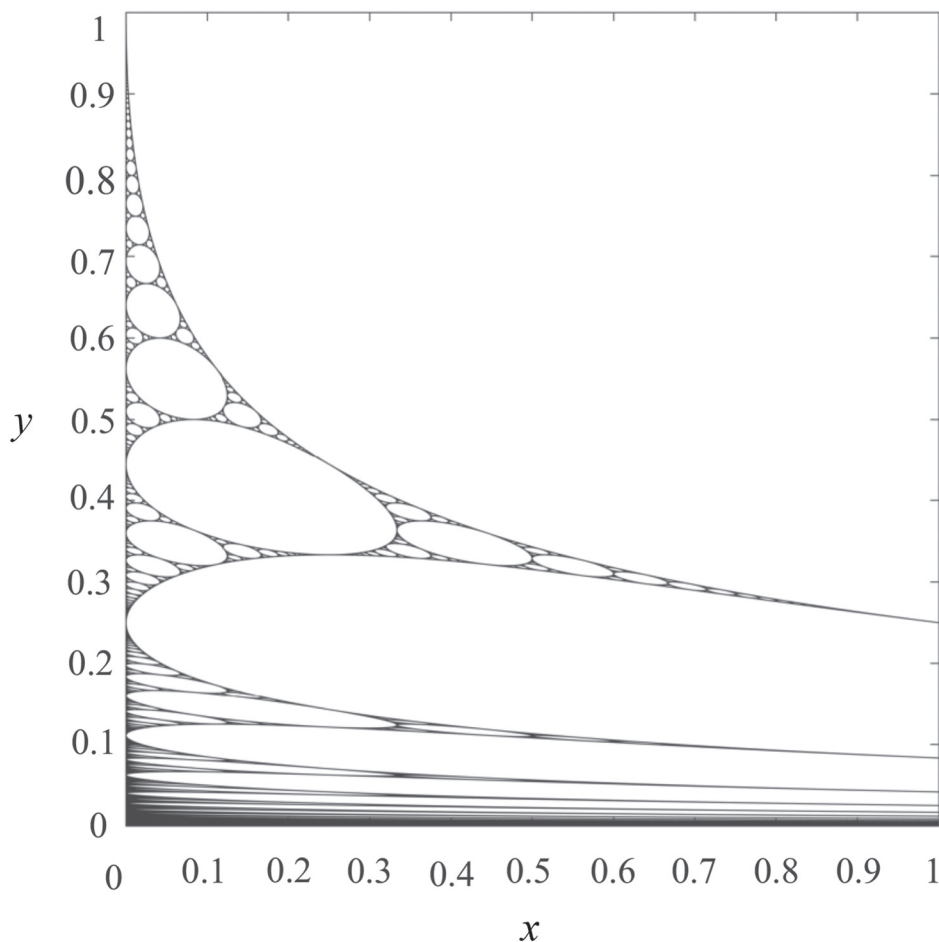


Figure 6. Picture answer: Types of packings that appear from triples of circles, or two circles and a line, as coded by their ratio pairs $(x, y) \in [0, 1] \times (0, 1]$. Points on curves and points on the y -axis are the ratio pairs that generate half-plane or strip packings. Points at intersections of curves and/or the y -axis are the ratio pairs that generate strip packings, and all other points on the curves and y -axis generate half-plane packings. Points in the delineated oval and partial-oval regions, which include their $x = 1$ and $y = 1$ edges, are the ratio pairs that generate bounded packings. The remaining points, which form a fractal, are the ratio pairs that generate full-plane packings.

Figure 4, and noticing that if a ratio pair on a curve moves slightly into a bordering oval or partial-oval region, then the associated triple adjusts in such a way to cause the bottom line in Figure 4 to bend and surround the packing. For example, the curves at the lower edges of the partial ovals are associated with triples that include A and B in Figure 4, and slightly increasing y into a partial-oval region means increasing the size of the triple's smallest circle, which then "pushes down" the circles between A and B , bending the bottom line into a surrounding circle. A proof along these lines would admittedly be cumbersome, but another piece of evidence is the fact that strip packings almost always turn into bounded packings upon slight changes in ratio pairs, and similarly, ratio pairs at intersections of curves in the plot almost always move into

oval or partial oval regions when changed slightly. Another approach that provides a proof can be found in [Section 5](#), which presents an alternative development of the plot.

Full-plane packings are given by the mysteriously interspersed remaining points. These are investigated in [Sections 5](#) and [6](#).

In fact, the entire plot invites further investigation. [Sections 5](#) and [6](#) provide a few results, as well as a springboard for additional exploration.

5. GENERAL STRUCTURE OF THE PICTURE. Certain facts about the overall structure of the ratio-pair plot, [Figure 6](#), can be proved most easily using a projective geometry approach, outlined here. In particular, this section proves that the set of points that give full-plane packings is a fractal, in the classical sense of having nonintegral Hausdorff dimension.

Apollonian packings can be considered to lie in the extended complex plane, $\mathbb{C}_\infty = \mathbb{C} \cup \infty$. Lines in \mathbb{C} are called “circles” in \mathbb{C}_∞ , so all Apollonian packings are comprised of circles here. The term *projective trio* will mean a set of three such pairwise tangent circles. It turns out that Apollonian packings are mapped to each other by Möbius transformations of \mathbb{C}_∞ ,

$$f(z) = \frac{az + b}{cz + d} \text{ with } a, b, c, d \in \mathbb{C} \text{ and } ad - bc \neq 0,$$

which take circles to circles. Because a Möbius transformation can be specified by its effect on three points, a projective trio can be mapped to any other projective trio by sending the three points of tangency in the first to those in the second. In addition, when applying a Möbius transformation to an Apollonian packing, the point p sent to ∞ determines the type of the resulting packing: If p lies on a circle, then the result is a strip or half-plane packing, depending on whether p is a point of tangency of two circles, or not, respectively. If p lies in one of the open disks, then the result is a bounded packing. If p is in the remaining fractal set, then the result is a full-plane packing.

This information suggests a way to answer the question, “What type of Apollonian packing will appear?” Given three circles that are pairwise externally tangent, perhaps a Möbius transformation could be found from a projective trio in a known Apollonian packing to that set of three circles, and the resulting type could be determined by the point p sent to ∞ . However, this attempt fails because determining the location of p relative to the circles in the known packing is essentially equivalent to the original problem.

Instead, it is possible to aim for an answer in the form of a picture—which turns out to be [Figure 6](#)—by using the idea of ratio pairs: Fix an Apollonian packing and one of its projective trios, and plot the ratio pairs of the image of the trio under a well-chosen set of Möbius transformations, as demonstrated here by way of an example. One nice combination is a strip packing with the trio shown in [Figure 7](#), along with the set of Möbius transformations consisting of those that fix 0 and 2, and whose points p sent to ∞ satisfy $p \in S$ where $S = \{z \in \mathbb{C} : 0 \leq \operatorname{Re}(z) \leq 1, \operatorname{Im}(z) < 0, |z| \geq 2\}$. This combination results in the bijection described by [Theorem 5.2](#) from S to the ratio pair space, $[0, 1] \times (0, 1]$.

Lemma 5.1. *Given a triple $\{A, B, C\}$ in Euclidean space, let a be the distance between the points where A is tangent to each of B and C ; similarly let b be the distance between B ’s points of tangency, and correspondingly c for C . Then the*

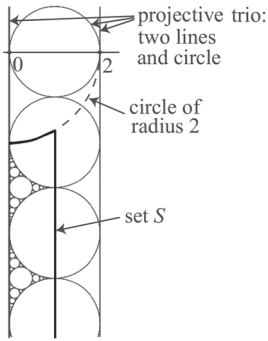


Figure 7. Example projective trio, Apollonian packing (only the portion inside S shown in detail), and set S for the Möbius transformation approach to the ratio-pair plot.

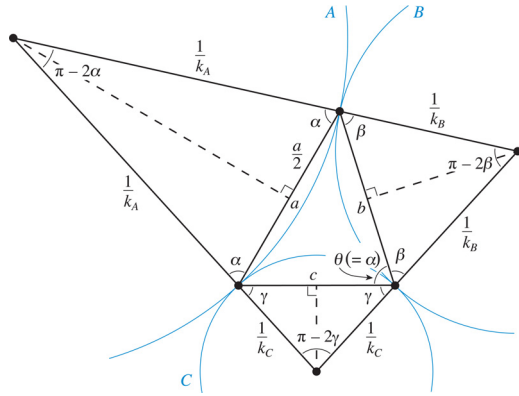


Figure 8. Illustration for Lemma 5.1. Given the distances a , b , and c between the points of tangency of circles A , B , and C , the curvatures k_A , k_B , and k_C can be determined.

curvatures k_A , k_B , and k_C of A , B , and C , respectively, are

$$k_A = \frac{-a^2 + b^2 + c^2}{abc}, \quad k_B = \frac{a^2 - b^2 + c^2}{abc}, \quad k_C = \frac{a^2 + b^2 - c^2}{abc}.$$

Proof. If the given triple $\{A, B, C\}$ does not contain a line, then let α , β , and γ be the angles indicated in Figure 8. Consequently, $(\pi - 2\alpha) + (\pi - 2\beta) + (\pi - 2\gamma) = \pi$ from the triangle formed by the centers of the circles, so $\alpha + \beta + \gamma = \pi$. Therefore in Figure 8, $\theta = \alpha$. The triangle whose vertices are the points of tangency thus has

$$a^2 = b^2 + c^2 - 2bc \cos(\alpha).$$

Meanwhile, $\cos(\alpha) = (a/2)k_A$ from the right triangle with hypotenuse $1/k_A$, and making this substitution for $\cos(\alpha)$ leads to the equation for k_A in the statement of the lemma. The equations for k_B and k_C are analogous.

If the triple contains a line — say C — then the equations for k_A and k_B follow by almost exactly the same reasoning but using $\gamma = \pi/2$ and replacing the lines through the center of C with parallel lines. The equation for k_C correctly gives $k_C = 0$. ■

Theorem 5.2. Let $S = \{z \in \mathbb{C} : 0 \leq \operatorname{Re}(z) \leq 1, \operatorname{Im}(z) < 0, |z| \geq 2\}$, and for each $p \in S$ let

$$f_p(z) = \frac{(2-p)z}{z-p},$$

i.e., the Möbius transformation that fixes 0 and 2, and sends p to ∞ . Let (x_p, y_p) be the ratio pair of the triple consisting of the images of the members of the projective trio shown in Figure 7: line $\operatorname{Re}(z) = 0$, line $\operatorname{Re}(z) = 2$, and circle $|z - 1| = 1$. Then the map $g : S \rightarrow [0, 1] \times (0, 1]$ defined by $g(p) = (x_p, y_p)$ is a bijection. Specifically,

$$g(p) = \left(\frac{p_1}{2 - p_1}, \frac{2(2 - p_1)}{-2p_1 + |p|^2} \right), \quad (4)$$

where $p = p_1 + ip_2$.

Proof. First, fix $p \in S$. To show that the ratio pair (x_p, y_p) is given by (4), let A , B , and C be the images under f_p of line $\operatorname{Re}(z) = 0$, line $\operatorname{Re}(z) = 2$, and circle $|z - 1| = 1$, respectively. The points of tangency, 0, 2, and ∞ , of these two lines and circle are mapped by f_p to 0, 2, and $2 - p$, respectively, which are therefore the points of tangency of A , B , and C : $2 - p$ for A and B , 0 for A and C , and 2 for B and C . Application of Lemma 5.1 leads to the circles' curvatures,

$$k_A = \frac{2p_1}{|p(2-p)|}, \quad k_B = \frac{2(2-p_1)}{|p(2-p)|}, \quad k_C = \frac{-2p_1 + |p|^2}{|p(2-p)|}.$$

Hence, equation (4) gives the ratio pair (x_p, y_p) .

Second, the map given by equation (4) is easily seen to be a bijection from S to $[0, 1] \times (0, 1]$: The parts of S 's boundary along $\operatorname{Re}(z) = 0$, $\operatorname{Re}(z) = 1$, and $|z| = 2$ map, respectively, to the $x = 0$, $x = 1$, and $y = 1$ parts of the boundary of $[0, 1] \times (0, 1]$. In addition, on the domain, the first expression of the pair in equation (4) is strictly monotonic in p_1 , while the second expression is strictly monotonic in p_2 with a limit of 0. ■

As a practical matter, actually creating a plot using this approach requires more background machinery and computation than does the approach of Sections 3 and 4, but the map given by equation (4) provides a visual relationship between the set S in the Apollonian packing (Figure 7) and the resulting plot of ratio pairs (Figure 6). Especially relevant is that the regions in Figure 6 delineated by the ovals and partial ovals are the images of the full and partial open disks in S in Figure 7, proving the statement in Section 4 that those regions in Figure 6 give bounded packings. In addition, a deeper excursion into the equations can give another proof that the curves are algebraic, this time looking at whole ovals.

Proofs about fractal dimension also become accessible. As background: The term *Apollonian gasket* is often used in the study of dimension to mean the complement of the set of open disks of an Apollonian packing confined to the curvilinear triangle bounded by three tangent circles. Apollonian gaskets are fractals in the classic sense of having nonintegral Hausdorff dimension. Every Apollonian gasket has the same Hausdorff dimension, proved in the 1960s to be nonintegral [13, 21], and eventually shown after some progressively precise bounds to have value ≈ 1.306 [20, 26]. Note that this value is smaller than the Sierpiński gasket's Hausdorff dimension, $\ln 3 / \ln 2 \approx 1.585$. Another relevant fact is that for a set $G \subseteq \mathbb{R}^n$, if $f : G \rightarrow \mathbb{R}^m$ is a bijection such that both f and f^{-1} satisfy Lipschitz conditions, then the Hausdorff dimension of $f(G)$ equals that of G [8].

Theorem 5.3. *In the ratio-pair plot of Figure 6, let H be the complement of the set consisting of the oval-shaped and partial-oval regions, which include their $x = 1$ and $y = 1$ boundary segments except for endpoints at parametric curves. Then H has Hausdorff dimension equal to that of an Apollonian gasket, i.e., approximately 1.306.*

Proof. Consider the Apollonian packing in Figure 7 to be in \mathbb{R}^2 , in the obvious way. Let $R \subseteq \mathbb{R}^2$ be analogous to S ; i.e., $R = \{(x, y) \in \mathbb{R}^2 : 0 \leq x \leq 1, y < 0, x^2 + y^2 \geq 4\}$. Let $h : R \rightarrow [0, 1] \times (0, 1]$ be analogous to g as given by equation (4); i.e., the equation for $h(x, y)$ is given by (4) with p_1 and $|p|^2$ replaced by x and $x^2 + y^2$, respectively. From Theorem 5.2 we can deduce that h is a bijection.

As seen in Figure 7, the set R contains a sequence of the packing's Apollonian gaskets G_n , $n = 1, 2, 3, \dots$, such that for each n , G_n spans from $x = 0$ to $x = 1$,

and $G_n \subseteq R_n$, where $R_n = \{(x, y) : 0 \leq x \leq 1, -(2n + 2) \leq y \leq -2n\}$. Note that $H = \bigcup_{n \in \mathbb{Z}^+} h(G_n)$. Write $h = (h_x, h_y)$. For fixed $n \in \mathbb{Z}^+$, it follows from the equation for h that the function h restricted to G_n satisfies a Lipschitz condition, and its inverse satisfies a Lipschitz condition, because there exist intervals $[x_1, x_2]$ and $[y_1, y_2]$ not containing 0 such that at every point in R_n , $\partial h_x / \partial x \in [x_1, x_2]$ and $\partial h_y / \partial y \in [y_1, y_2]$ while $\partial h_y / \partial x$ is bounded and $\partial h_x / \partial y = 0$.

Since H is a countable union of these images $h(G_n)$ of Apollonian gaskets, the dimension of H equals that of an Apollonian gasket. ■

Corollary 5.4. *The set F of ratio pairs that generate full-plane packings has Hausdorff dimension equal to that of an Apollonian gasket, i.e., approximately 1.306.*

Proof. Let H be as in [Theorem 5.3](#). The set difference between H and F has Hausdorff dimension 1 because it is comprised of a countable collection of 1-dimensional pieces of algebraic curves. Therefore, since the Hausdorff dimension of H is greater than 1, it is equal to that of F . ■

An interesting consequence is a hierarchy among the four types of packings: Strip packings, half-plane packings, full-plane packings, and bounded packings have sets of ratio pairs with respective Hausdorff dimensions 0, 1, ≈ 1.306 , and 2.

6. BEGINNING OF THE EXPLORATION. The picture answer of [Figure 6](#) suggests a number of questions. What characterizes various portions of the plot? What is the pattern relating the locations of curves in the plot to the positions of their parametric triples in the Apollonian packing as displayed in [Figure 4](#)? More generally, how do locations in $[0, 1] \times (0, 1]$ relate to positions in a packing?

Questions also arise about specific Apollonian packings. Given a packing, what does its set—i.e., its *equivalence class*—of ratio pairs of triples look like in the picture? Is there a pattern within and/or between equivalence classes?

This section forms just the beginning of an exploration, and introduces additional open questions as well.

The strip packing. We already know that there is only one strip packing up to similarity. Therefore, there is only one equivalence class, which consists of the intersections between curves and/or the y -axis.

This fact can be viewed in relation to the known [Propositions 2.2](#) and [2.3](#) about the strip packing and rational points. [Proposition 2.2](#) tells us that all intersections occur at rational points. [Proposition 2.3](#) states a further restriction for curves' intersections with the y -axis, namely that they occur at *squares* of rational points. This proposition has an immediate interpretation if the picture is re-done in terms of square roots of the coordinates, as in [Figure 9](#): The curves intersect the vertical axis at exactly the rational points.

In fact, the appearance of these rational intersections with the vertical axis could be investigated in terms of Ford circles [\[9\]](#), i.e., those tangent to the line in the packing, and Farey fractions, for which an entertaining exposition can be found in [\[27\]](#).

Half-plane packings. A first observation about half-plane packings is that each oval in [Figure 6](#) is comprised of six curves from a *sextuplet* of parametric triples, as shown in [Figure 10](#). The reason that these sets of curves make loops is explained here; the resulting shapes being “ovals” is simply an observation from [Figure 6](#). In the top half of [Figure 10](#), triples that are mirror images across the vertical dashed line have the same ratio pair, so their curves begin (at $t = 0$) at the same point. Triples that are

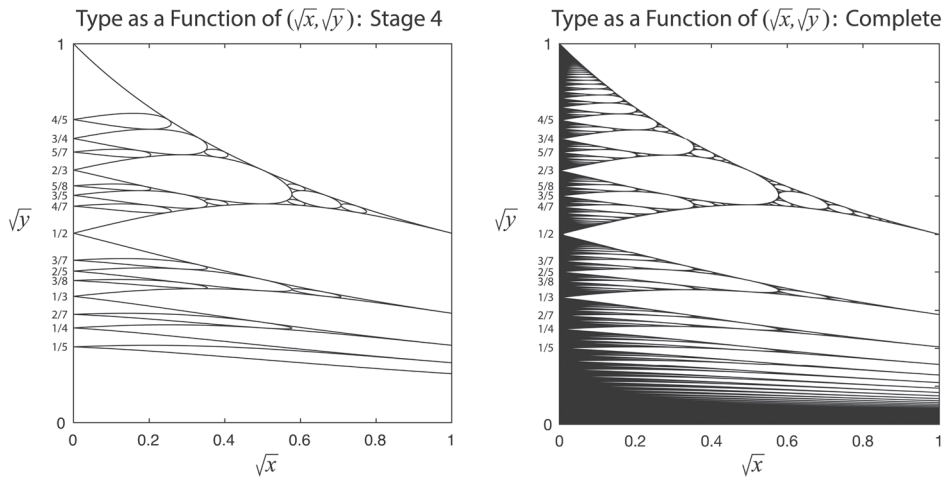


Figure 9. Same as Figure 5 (Stage 4) and Figure 6 (Complete) but with square root scaling so that intersections with the vertical axis are at exactly the rational points.

rough mirror images over the diagonal dashed curve have the same ratio pair at $t = 1$, so their curves end (at $t = 1$) at the same point. Therefore, traveling along successive parametric curves of a sextuplet creates a closed curve in the ratio-pair plane.

Not every parametric triple is a member of a sextuplet, as can be seen by looking at triples in Figure 10. Each nonsextuplet triple includes at least two of $A(t)$, B , and $C(t)$, and is symmetric (roughly) over a dashed line or curve. In the ratio-pair plot, these triples produce the long curves that begin at $x = 0$ and $x = 1$, such as those labeled in Figure 5, Stage 2, because the ratio of curvatures between any two of $A(0)$, B , and $C(0)$ is 0 or 1.

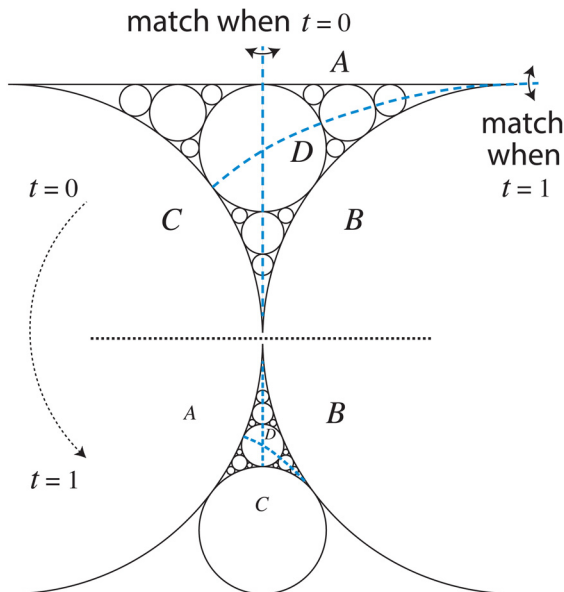


Figure 10. In the notation of Figure 4, the symmetries that cause parametric triples' ratio pairs to match when $t = 0$ and $t = 1$. Except for triples containing at least two of $A(t)$, B , and $C(t)$, each parametric triple belongs to a sextuplet determined by reflections over the dashed curves in alternation.

These long curves delineate a sequence of curvilinear triangular full-width portions of the plot in Figure 6, and a natural question arises: For each such triangular region, what characterizes the parametric triples that produce the curves inside that region? The answer is that the top triangular region corresponds to triples in which the two smallest circles are from consecutive generations of the development of the Apollonian packing in Figure 4 beginning with 0th generation $\{A(t), B, C(t)\}$, and the n th region from the top corresponds to triples in which the two smallest circles are from generations that are n apart. This answer could be proved formally using reasoning about connections between curves. Intuitively, the answer makes sense because larger differences between generations mean smaller ratios and thus smaller values of y .

More specifically, we can ask: Which curves in Figure 6 correspond to which parametric triples in Figures 4 or 10? Except for a few special cases, this question is left open here. Particularly interesting would be a thorough guide to the plot. One key is that curves connect not just at mutual $t = 0$ or $t = 1$ points, but also at other points. For example, a “ $t = 1$ ” triple in the bottom half of Figure 10 has the same ratio pair as two triples between B, C , and D in the top half. Thus, two new curves begin ($t = 0$) at the $t = 1$ end of the original curve. In addition, curves intersect at values of t besides 0 and 1.

Regarding the equivalence class for a given half-plane packing: Since each half-plane packing is represented in Figure 4 for some value of $t \in (0, 1)$, say t_0 , we know that every one of Theorem 3.5’s parametric triples will generate the given half-plane packing when $t = t_0$. Because each oval in the plot is created by a sextuplet of these parametric triples, an oval will get exactly six points of the equivalence class from its six parametric triples with $t = t_0$. Meanwhile, a given half-plane packing has many tents, and each tent is equivalent to $\{A(t), B, C(t)\}$ for some t in Figure 4. Thus there are many values of t that can be used to produce the same packing. In the end, each oval includes infinitely many sets of six points of the equivalence class.

Bounded packings. Two observations are made here about bounded packings. The first is that the partial-oval regions correspond to triples with at least two circles tangent to the bounding circle. This fact is deduced from the development in Section 4: The lower edges of the partial ovals stem from Figure 4’s parametric triples that have largest two circles $A(t)$ and B , as that pair produces ratio x spanning from 0 to 1. As mentioned in Section 4, slightly increasing y from a specific such triple, say with $t = t_0$, creates a bounded packing because the bottom line becomes the surrounding circle. Relevant here is that $A(t_0)$ and B become tangent to the bounding circle. An alternative explanation is provided by the viewpoint of Section 5: The partial-oval regions correspond to parts of disks in Figure 7 that have their boundary circles tangent to both lines. When a point p in such a disk is sent to ∞ , its surrounding circle becomes the packing’s bounding circle, which is then tangent to the images of the two lines (these images being members of the triple).

The second observation is about equivalence classes, particularly within the topmost partial-oval region. Application of the reasoning above shows that this region corresponds to triples with all three circles tangent to the bounding circle. Each bounded packing has a countably infinite number of triples tangent to the bounding circle, with a countably infinite number of ratio pairs. Therefore, within the topmost partial-oval region, each equivalence class is countably infinite. Conveniently, nevertheless, there is a canonical set of representatives for the equivalence classes: the ratio pairs of the triples of largest three circles (besides the bounding circle) in a packing. This canonical set is shown in Figure 11.

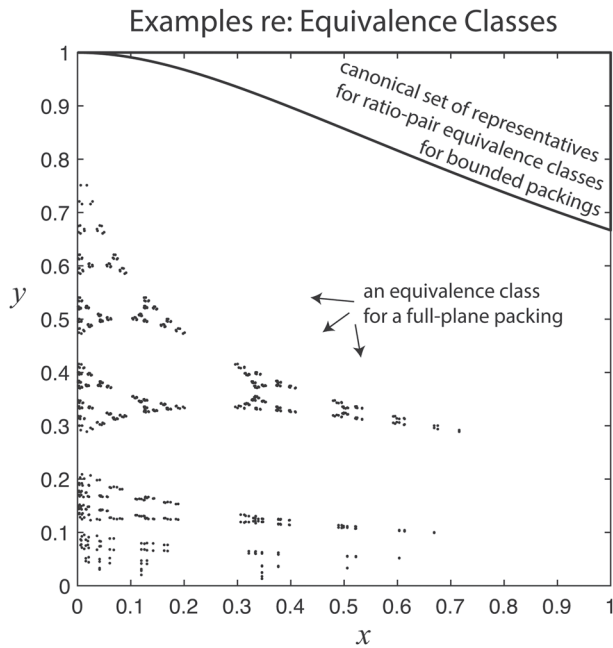


Figure 11. Examples regarding equivalence classes. The closed set outlined at the top is a canonical set of representatives for bounded packings. The set of dots shows 1,093 of the infinitely many ratio pairs that generate the full-plane packing in Figure 2.

In fact, there are many canonical sets of representatives. One collection is based upon the fact that it is possible to specify the positions of all triples in relation to the largest three circles.

Full-plane packings. The ratio pairs for full-plane packings are hiding in the fractal between the curves. How do we “find” these points? The answer is to use a classic method: Construct sequences whose limits are guaranteed to not be anywhere else.

We can construct these sequences from endpoints of successive parametric curves, using the stages as illustrated in Figure 5. More precisely, choose a curve and travel to its $t = 1$ endpoint, then choose one of the adjoining next-stage curves and travel to its $t = 1$ endpoint, and so on. The limit of the sequence will be bounded away from every curve as long as the following holds: For every step in the sequence, there exists a later step in which the chosen next-stage curve begins in the direction opposite to that traveled to the end of the previous curve. The limit is then a ratio pair that generates a full-plane packing, because the point is not on a curve, and is not in an open set disjoint from all of the curves.

Figure 12 shows an example in which the direction changes at every endpoint. In this example, it turns out that the triples are equivalent to those formed from consecutive circles in a spiral as shown at right in Figure 12. The limit of this sequence of ratio pairs is $(\phi - \sqrt{\phi}, \phi - \sqrt{\phi})$, which corresponds to the self-similar full-plane packing discussed in Section 2 and shown in Figure 2.

Another way to find ratio pairs that generate full-plane packings is to use a related idea with the alternative approach of Section 5. In the set S of Figure 7, travel along a sequence of arcs through successive stages of smaller and smaller circles, changing directions occasionally. Applying the map in equation (4) to the limit will produce a ratio pair that generates a full-plane packing.

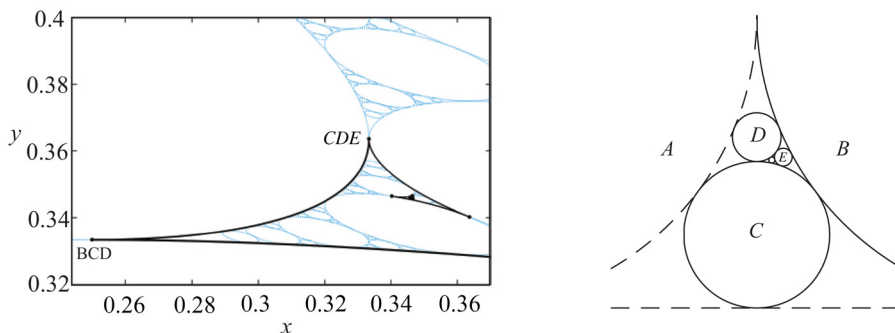


Figure 12. Left: A sequence of ratio pairs whose limit generates a full-plane packing. The sequence is given by the endpoints of the solid parametric curves, while the dotted curves are shown for reference in relation to Figure 6. Right: The clockwise spiral of circles starting with B, C, D, E , based on Figure 4 using $t = 1$, whose consecutive-circle triples are those that produce the solid parametric curves at left. The ratio pairs of the first two triples are labeled at left.

What do equivalence classes look like? Figure 11 provides an example. The points in Figure 11 were calculated from triples in the full-plane packing, rather than by taking limits of sequences; open for investigation is the question of which sequences have limits that give the same full-plane packing.

More questions. The reader can probably imagine many more questions and directions for exploration than would fit here. More questions could be asked about equivalence classes, for example about canonical sets of representatives, as well as about patterns within and/or between equivalence classes. Additional investigation is possible on the topic of algebraic curves. More features of the plot could be explored, for example from the viewpoints of geometry or analysis.

While the approach of Sections 3 and 4 provides the most direct relationship between specific trios and types of packings, the alternative approach of Section 5 inspires its own host of questions. An inquiry could begin with various sets and projective trios, as in Figure 7, for which a well-chosen set of Möbius transformations leads to a bijective map to the ratio-pair space $[0, 1] \times (0, 1]$. An interesting next step might be a graphical display to show the manner in which an entire packing repeatedly covers the ratio-pair space with such a map.

Another enticing idea, with either approach, is to use animations to illustrate results. How do ratio pairs, or sets of ratio pairs, move through the plot as the triples and packings deform in systematic ways? Or the converse: How does a packing change as a triple's ratio pair follows a path of interest? These questions are just a tip of the iceberg.

ACKNOWLEDGMENTS. The author thanks Gerardo Lafferriere of the Fariborz Maseeh Department of Mathematics and Statistics at Portland State University for the welcome to PSU as a Visiting Scholar during a portion of this project, and thanks anonymous reviewers for helpful comments among which was the information about reference [2]. This work received support from the Colby College Research Grant Program.

ORCID

Jan E. Holly <http://orcid.org/0000-0002-6419-3038>

REFERENCES

- [1] Aharonov, D., Stephenson, K. (1998). Geometric sequences of discs in the Apollonian packing. *St. Petersburg Math. J.* 9(3): 509–542.
- [2] Bos, E.-J. (2010). Princess Elizabeth of Bohemia and Descartes' Letters (1650–1665). *Historia Math.* 37(3): 485–502.
- [3] Bourgain, J., Kontorovich, A. (2014). On the local-global conjecture for integral Apollonian gaskets. *Invent. Math.* 196: 589–650. With an appendix by Péter P. Varjú.
- [4] Ching, M., Doyle, J. R. (2012). Apollonian circle packings of the half-plane. *J. Comb.* 3(1): 1–48.
- [5] Cox, D. A., Little, J., O'Shea, D. (2005) *Using Algebraic Geometry*, 2nd ed. New York, NY: Springer.
- [6] Coxeter, H. S. M. (1968). The problem of Apollonius. *Amer. Math. Monthly.* 75(1): 5–15.
- [7] Coxeter, H. S. M. (1989). *Introduction to Geometry*, 2nd ed. New York, NY: John Wiley & Sons.
- [8] Falconer, K. (2014). *Fractal Geometry: Mathematical Foundations and Applications*. Chichester, West Sussex, UK: John Wiley & Sons.
- [9] Ford, L. R. (1938). Fractions. *Amer. Math. Monthly.* 45(9): 586–601.
- [10] Fuchs, E. (2013). Counting problems in Apollonian packings. *Bull. Amer. Math Soc. (N.S.)*, 50(2): 229–266.
- [11] Graham, R. L., Lagarias, J. C., Mallows, C. L., Wilks, A. R., Yan, C. H. (2003). Apollonian circle packings: Number theory. *J. Number Theory.* 100: 1–45.
- [12] Graham, R. L., Lagarias, J. C., Mallows, C. L., Wilks, A. R., Yan, C. H. (2005). Apollonian circle packings: Geometry and group theory I. The Apollonian group. *Discrete Comput. Geom.* 34: 547–585.
- [13] Hirst, K. E. (1967). The Apollonian packing of circles. *J. London Math. Soc.* 42: 281–291.
- [14] Kasner, E. Supnick, F. (1943). The Apollonian packing of circles. *Proc. Nat. Acad. Sci. U.S.A.* 29: 378–384.
- [15] Kontorovich, A. (2013). From Apollonius to Zaremba: Local-global phenomena in thin orbits. *Bull. Amer. Math Soc. (N.S.)*, 50(2): 187–228.
- [16] Lagarias, J. C., Mallows, C. L., Wilks, A. R. (2002). Beyond the Descartes circle theorem. *Amer. Math. Monthly.* 109(4): 338–361.
- [17] Levrie, P. (2019). A straightforward proof of Descartes's circle theorem. *Math. Intelligencer.* 41(3): 24–27.
- [18] Mackenzie, D. (2010). A tisket, a tasket, an Apollonian gasket. *Am. Sci.* 98(1): 10–14.
- [19] *MATLAB*, Version 9.3 (R2017b). (2017). Natick, MA: The MathWorks, Inc.
- [20] McMullen, C. T. (1998). Hausdorff dimension and conformal dynamics, III: Computation of dimension. *Amer. J. Math.* 120(4): 691–721.
- [21] Melzak, Z. A. (1966). Infinite packings of disks. *Canad. J. Math.* 18: 838–852.
- [22] Oh, H. (2014). Apollonian circle packings: dynamics and number theory. *Jpn. J. Math.* 9: 69–97.
- [23] Pedoe, D. (1967). On a theorem in geometry. *Amer. Math. Monthly.* 74(6): 627–640.
- [24] Sarnak, P. (2011). Integral Apollonian packings. *Amer. Math. Monthly.* 118(4): 291–306.
- [25] Satija, I. I. (2016). *Butterfly in the Quantum World: The Story of the Most Fascinating Quantum Fractal*. San Rafael, CA: Morgan & Claypool Publishers.
- [26] Thomas, P. B., Dhar, D. (1994). The Hausdorff [sic] dimension of the Apollonian packing of circles. *J. Phys. A: Math. Gen.* 27: 2257–2268.
- [27] Tou, E. R. (2017). The Farey sequence: From fractions to fractals. *Math Horizons.* 24(3): 8–11.

JAN E. HOLLY is a mathematician who continues to be intrigued by interesting problems in pure mathematics while also doing research in applied mathematics. This interest in exploration apparently extends to geography as well, with an education and career that have included University of Colorado, University of New Mexico, University of Illinois (Ph.D. in mathematics with specialization in logic and algebra), Robert S. Dow Neurological Sciences Institute in Oregon (postdoc in mathematical neuroscience), Colby College in Maine, as well as stints at The Hebrew University of Jerusalem, Center for Computational Biology in Montana, and Santa Fe Institute in New Mexico.

Department of Mathematics and Statistics, Colby College, Waterville, ME 04901
Jan.Holly@colby.edu